

# High frequency variability of the Atlantic meridional overturning circulation

B. Balan Sarojini<sup>1,2</sup>, J. M. Gregory<sup>1,2,3</sup>, R. Tailleux<sup>2</sup>, G. R. Bigg<sup>4</sup>, A. T. Blaker<sup>5</sup>, D. R. Cameron<sup>6</sup>, N. R. Edwards<sup>7</sup>, A. P. Megann<sup>5</sup>, L. C. Shaffrey<sup>1,2</sup>, and B. Sinha<sup>5</sup>

<sup>1</sup>National Centre for Atmospheric Science – Climate Division, Reading, UK

<sup>2</sup>Walker Institute for Climate System Research, University of Reading, Reading, UK

<sup>3</sup>Met Office Hadley Centre, Exeter, UK

<sup>4</sup>Department of Geography, University of Sheffield, Sheffield, UK

<sup>5</sup>National Oceanography Centre, Southampton, UK

<sup>6</sup>Centre for Ecology and Hydrology, Edinburgh, UK

<sup>7</sup>Earth and Environmental Sciences, The Open University, Milton Keynes, UK

Received: 19 November 2010 – Published in Ocean Sci. Discuss.: 28 January 2011

Revised: 20 June 2011 – Accepted: 4 July 2011 – Published: 18 July 2011

**Abstract.** We compare the variability of the Atlantic meridional overturning circulation (AMOC) as simulated by the coupled climate models of the RAPID project, which cover a wide range of resolution and complexity, and observed by the RAPID/MOCHA array at about 26° N. We analyse variability on a range of timescales, from five-daily to interannual. In models of all resolutions there is substantial variability on timescales of a few days; in most AOGCMs the amplitude of the variability is of somewhat larger magnitude than that observed by the RAPID array, while the time-mean is within about 10% of the observational estimate. The amplitude of the simulated annual cycle is similar to observations, but the shape of the annual cycle shows a spread among the models. A dynamical decomposition shows that in the models, as in observations, the AMOC is predominantly geostrophic (driven by pressure and sea-level gradients), with both geostrophic and Ekman contributions to variability, the latter being exaggerated and the former underrepresented in models. Other ageostrophic terms, neglected in the observational estimate, are small but not negligible. The time-mean of the western boundary current near the latitude of the RAPID/MOCHA array has a much wider model spread than the AMOC does, indicating large differences among models in the simulation of the wind-driven gyre circulation, and its variability is unrealistically small in the models. In many

RAPID models and in models of the Coupled Model Inter-comparison Project Phase 3 (CMIP3), interannual variability of the maximum of the AMOC wherever it lies, which is a commonly used model index, is similar to interannual variability in the AMOC at 26° N. Annual volume and heat transport timeseries at the same latitude are well-correlated within 15–45° N, indicating the climatic importance of the AMOC. In the RAPID and CMIP3 models, we show that the AMOC is correlated over considerable distances in latitude, but not the whole extent of the North Atlantic; consequently interannual variability of the AMOC at 50° N, where it is particularly relevant to European climate, is not well-correlated with that of the AMOC at 26° N, where it is monitored by the RAPID/MOCHA array.

## 1 Introduction

Any substantial change, whether anthropogenic or natural, in the meridional overturning circulation of the Atlantic Ocean (AMOC) could considerably affect the climate, especially of the North Atlantic and Europe, on account of the associated northward ocean heat transport. A complete cessation of the AMOC would produce a strong cooling (Vellinga and Wood, 2002; Stouffer et al., 2006), but this is very unlikely during the 21st century according to the latest assessment of the Intergovernmental Panel on Climate Change (Meehl et al., 2007). Schmittner et al. (2005) and Meehl et al. (2007) show



Correspondence to: B. Balan Sarojini  
(b.balansarojini@reading.ac.uk)

that there exists a wide range of weakening – from 0% to 50% – of the AMOC by 2100 in model projections of climate change under scenarios of increasing anthropogenic greenhouse gas concentrations. Other studies (Knight et al., 2005; Keenlyside et al., 2008) suggest that AMOC may weaken over the next decade due to unforced (natural) variability, resulting in a cooler climate around the North Atlantic. The internally generated interannual variability of the AMOC in coupled AOGCMs (Dong and Sutton, 2001; Collins et al., 2006) and in ocean-alone GCMs (Biastoch et al., 2008) is found to be closely linked to interannual variations in Atlantic Ocean heat transport (AOHT). Understanding the unforced interannual variability of the AMOC and AOHT is important because it is the background against which any signal of climate change has to be detected.

Because of such considerations, the RAPID/MOCHA array (Cunningham et al., 2007; Kanzow et al., 2007, 2010; Bryden et al., 2009; Johns et al., 2011) was deployed at 26.5° N in the Atlantic Ocean to monitor the AMOC and provide information about its variability. The array data show temporal variability in the AMOC on a broad range of time scales, from interannual to daily. The latter part of the AMOC variability spectrum has not been much studied in the numerical models used for climate projections. The question thus arises of whether they are able to represent it realistically and if so, what the physical sources of the variability are.

The RAPID programme, which established the observational array, also includes an intercomparison project of UK global climate models (the RAPID models) of varying resolution and complexity. This study reports on that project and has two topics. In the first topic, we use the 5-yr-long RAPID/MOCHA dataset to evaluate and compare the RAPID models in regard to high-frequency variability, which is a new kind of observational information. In the second topic, we set the high-frequency observations at 26° N into their climatic context, by analysing the relationship between volume transport and heat transport at different timescales and at various latitudes in the North Atlantic. The connection between these topics, and the motivation for the study, is the dataset from the RAPID/MOCHA monitoring array at 26° N.

Model intercomparison is valuable for assessing model systematic uncertainty and to study its causes (e.g. Gregory et al., 2005; Stouffer et al., 2006; Griffies et al., 2009). The high-frequency AMOC variability simulated by two climate models is assessed in Baehr et al. (2009) using the first year of data from the RAPID array. They found that the magnitude of variability is well reproduced in ECHAM5/MPI-OM, and ECCO-GODAE shows significant correlation of the daily AMOC to that of the RAPID/MOCHA time series. ECHAM5/MPI-OM is an AOGCM whereas ECCO-GODAE is a data-assimilation product using an ocean-alone GCM. The ECCO-GODAE time series is expected to correlate to that of RAPID array because the model is forced

by NCEP/NCAR reanalysis fluxes for the one-year analysis period and prior to that the model solution is evolved using an optimised initial state from many observational datasets. Our study is able to use a longer observational timeseries and a wider range of models.

The common paradigm of the AMOC as a single, basin-scale, meridionally coherent zonally integrated circulation in the North Atlantic is challenged by recent studies (Bingham et al., 2007; Willis, 2010; Lozier et al., 2010). Therefore the representativeness of the transport measured at 26° N and its climatic impact on the higher latitudes is a key question to be addressed. From the climate science point of view, the main motivation for the RAPID monitoring array is the climatic influence of the AMOC and how it might change in the future, and we depend on models for information on the climatic influence of the AMOC on multiannual timescales.

## 2 Data – models and observations

### 2.1 Models

The RAPID-models, namely HadCM3, FAMOUS, FORTE, FRUGAL, GENIE, CHIME and HiGEM, are all global coupled atmosphere-ocean models without flux adjustments. They are all employed for investigations of climate variability and change on various timescales. The specifications of their atmosphere and ocean components are summarised in Table 1.

*HadCM3* (Gordon et al., 2000) is a Hadley Centre atmosphere–ocean general circulation model (AOGCM) which has been used successfully for many purposes and extensively cited, for instance in the IPCC Fourth Assessment Report. *FAMOUS* (Jones et al., 2005; Smith et al., 2008) is a low-resolution version of HadCM3, calibrated to replicate HadCM3 climate as closely as possible. It runs ten times faster than HadCM3, making it a computationally less expensive AOGCM for long-term or large ensembles of climate simulations. *HiGEM* (Shaffrey et al., 2009) is a high-resolution AOGCM derived originally from the Hadley Centre AOGCM HadGEM1. Compared to HadCM3, the predecessor of HadGEM1, HiGEM has new atmospheric and sea-ice dynamics submodels together with substantial differences in the ocean such as a linear-free surface, a 4th order advection scheme, 40 vertical levels and the Gent-McWilliams mixing scheme being turned off. It has an eddy-permitting ocean and allows fine spatial and temporal coupling between the ocean and atmosphere. HiGEM is computationally expensive but several multi-decadal runs with it have been completed. *FORTE* (Blaker et al., 2011) uses a recoded version (MOMA, Webb, 1996) of the Modular Ocean Model (MOM) (Pacanowski, 1990). It is similar to that of the Hadley Centre models and is at a resolution between the HadCM3 and FAMOUS ocean, but has a spectral atmospheric dynamics submodel with higher resolution than the HadCM3 atmosphere,

**Table 1.** Specifications of the RAPID-models; time-mean and standard deviations (X(Y) indicates X is mean and Y is SD) of simulated Atlantic Ocean meridional overturning transport (in Sv),  $T_{\text{over}}$ , at  $26^\circ$  N and of the maximum of Atlantic MOC,  $M_{\text{max}}$  on 5-daily and annual timescales; time-mean and standard deviation (SD) of the simulated 5-daily  $T_{\text{over}}$ ,  $29^\circ$  N and its decomposed components ( $T_{\text{Ek}}$ : Ekman part,  $T_{\text{geo}}$ : geostrophic part,  $T_{\text{vis}}$ : viscous/frictional part and  $T_{\text{adv}}$ : advection part); time-mean of simulated annual Atlantic Ocean meridional heat transport (AOHT in PW),  $26^\circ$  N and the interannual correlation  $T_{\text{over}}$  at  $26^\circ$  N with  $M_{\text{max}}$ , AOHT at  $26^\circ$  N and AOHT at  $50^\circ$  N. The RAPID/MOCHA observational estimate (of 5 yr) is given in the last column. The observed geostrophic transport is the sum of the mid-ocean transport and Florida current transport. The 1-yr statistics given for the 5-daily  $T_{\text{over}}$ , at  $26^\circ$  N, is for the second year of the model integrations and the observations. In HiGEM and FORTE, the transport component due to viscous part has 2 parts namely, by the Laplacian and biharmonic terms. In FORTE, the biharmonic term is implicit and could not be calculated offline. The FRUGAL transport at  $26^\circ$  N is calculated along a curvilinear gridline which is near  $26^\circ$  N. Time-step data is used in GENIE which has an ocean time-step of 3.65 days. GENIE and FRUGAL have no seasonal variability in wind-stress and no interannual variability. The Gulf Stream component ( $T_{\text{GS}}$ ) is not part of the physical decomposition; it is estimated geographically (see Sect. 4 for details). Meridional correlation length (in  $^\circ$ lat) at  $26^\circ$  N is defined as the latitudinal extent of positive correlation above 0.5 in both directions. FRUGAL and CHIME data are only available for some of the calculations.

Model	HadCM3	FAMOUS	FRUGAL	FORTE	GENIE	CHIME	HiGEM	OBS
Atmos res: lon $\times$ lat $\times$ level	$3.75 \times 2.5 \times 19$	HadCM3 at $7.5 \times 3.75 \times 11$	Enhanced UVic	IGCM3 T42 $\times$ 15	UVic 2D	HadCM3 atmos	HadGEM1 at $1.25 \times$ $0.83 \times 38$	
Ocean res: lon $\times$ lat $\times$ level	$1.25 \times 1.25 \times 20$	HadCM3 at $3.75 \times 2.5 \times 20$	MOM V2 with high-res Arctic	MOM 2 $\times$ 2 $\times$ 15	GOLDSTEIN $10 \times 5 \times 8$	HYCOM at $1.25 \times 1.25 \times 25$	HadGEM1 at $0.33 \times$ $0.33 \times 40$	
<i>T<sub>over</sub></i> (Sv)								
Latitude $^\circ$ N/Depth(m)	26.3/995	26.3/995		26.0/1365	26.4/1158	26.3/1050	26.9/959	26.5/1041
5-daily, 1 yr	18.8 (4.3)	19.0 (4.2)	25.9 (1.2)	16.4 (4.2)	16.4 (0.3)	15.4 (3.3)	15.1 (2.6)	19.5 (5.3)
5-daily, 10 yr	17.1 (4.1)	18.2 (4.2)	26.4 (1.4)	17.2 (4.5)	16.4 (0.3)	15.0 (3.3)	15.5 (4.0)	18.6 (4.5)
annual	16.8 (0.9)	20.6 (1.3)		17.6 (1.1)	16.5 (0)	18.8 (1.2)	16.4 (1.0)	
<i>M<sub>max</sub></i> (Sv)								
5d–10 yr	21.9 (2.4)	18.7 (3.0)	26.5 (1.3)	21.3 (2.5)	18.5 (0.3)		20.6 (2.5)	
annual	18.9 (0.7)	20.0 (1.3)		19.8 (1.1)	18.6 (0)	20.1 (1.7)	18.9 (1.1)	
Dynamical decomposition of <i>T<sub>over</sub></i> (Sv) for 5-daily means (except time-step for GENIE and geographical estimate for <i>T<sub>GS</sub></i> )								
Latitude $^\circ$ N/Depth(m)	28.8/995	28.8/995		30/1365	30/1158		28.9/959	26.5/1041
Overturning <i>T<sub>over</sub></i>	18.0 (4.3)	18.1 (3.7)		16.5 (3.9)	16.1 (0.1)		15.7 (3.6)	18.6 (4.5)
Ekman <i>T<sub>Ek</sub></i>	0.9 (4.0)	3.5 (3.5)		1.4 (3.8)	−2.3 (0)		1.6 (3.3)	3.6 (3.2)
Geostrophic <i>T<sub>geo</sub></i>	17.6 (2.3)	15.3 (1.6)		15.2 (2.8)	16.8 (0.1)		14.4 (2.6)	15.0 (3.5)
Viscous <i>T<sub>vis</sub></i>	−0.4 (0.1)	−0.8 (0.2)		−0.1(0.1)	1.7 (0.0)		0.0 (0.0), −0.1 (0.1)	
Advective <i>T<sub>adv</sub></i>							0.3 (0.6)	
Correlation( <i>T<sub>int</sub></i> , <i>T<sub>ext</sub></i> )	−0.98	−0.94		−0.64			−0.96	−0.83
Gulf Stream <i>T<sub>GS</sub></i>	43.5 (4.1)	21.2 (1.4)	48.1 (2.2)	16.9 (1.4)	22.1 (0.14)	13.2 (2.1)	16.7 (1.7)	31.9 (3.0)
Latitudinal variation of annual volume and heat transport								
Corr. length ( $^\circ$ lat), $26^\circ$ N	40	24		25			28	
Latitude of <i>M<sub>max</sub></i> ( $^\circ$ N)	35–45	31–34		30–40	46–51	23–60	34–45	
Corr ( <i>T<sub>over</sub></i> $_{26^\circ}$ N, <i>M<sub>max</sub></i> )	0.38	0.96		0.70	0.93	0.53	0.74	
Mean AOHT, $26^\circ$ N (PW)	1.0	0.8		1.1			1.1	
Corr ( <i>T<sub>over</sub></i> , AOHT), $26^\circ$ N	0.8	0.8		0.9			0.9	
Corr ( <i>T<sub>over</sub></i> $_{26^\circ}$ N, AOHT $_{50^\circ}$ N)	0.00	0.24		0.39		0.42	0.36	

and simpler atmospheric physics. *CHIME* (Megann et al., 2010) couples the atmosphere model of HadCM3 with a predominantly isopycnic ocean (hybrid-coordinate ocean, HYCOM; Bleck, 2002), the only RAPID-model using such a scheme rather than horizontal levels of fixed depth. *FRUGAL* (Bigg and Wadley, 2001) has an energy-moisture balance advective-diffusive atmospheric component, based on the UVic model of Weaver et al. (2001). It does not simulate winds, and a prescribed wind-stress climatology is applied to the ocean. *FRUGAL* uses the MOM ocean with a grid designed to improve resolution of the Arctic Ocean. *GENIE* (Edwards and Marsh, 2005) also uses the UVic atmosphere and is the only RAPID-model which does not have a primitive-equation ocean model; instead, it uses a frictional geostrophic model (GOLDSTEIN) in which horizontal momentum diffusion is parameterised by Rayleigh friction

rather than viscosity. This is computationally very cheap and consequently GENIE is the fastest RAPID-model by a large factor, suiting its intended use for multimillennial climate simulations and very large ensembles.

For this analysis, we produced 10 yr of 5-daily model data (i.e. 5-day means) from the unforced control integrations of the models. Control integrations are customarily evaluated with respect to present-day climatology, especially for internal variability. This simplifies comparison of model and observational results by avoiding the complications of whether radiative forcings of climate change are the same in different climate models and whether trends associated with climate change are realistically simulated. For calculation of the interannual variability of the simulated AMOC, we also produced timeseries of 110 yr of annual means from the control integrations. The data analysed in this paper comes from

portions of the control runs after the models have been spun up for many hundred years except in HiGEM and CHIME where the control runs are only 115 and 200 yr long, respectively. The 5-daily data in CHIME and HiGEM is from year 60 to year 70. The annual data in CHIME is from year 60 to year 170, and in HiGEM from year 20 to year 110, only 90 yr long, after a short spin-up time.

## 2.2 Observations

The RAPID/MOCHA array is the first system able to monitor a basin-wide transport at a latitude continuously. It is designed to estimate the AMOC as the sum of three observable components namely, Ekman transport, Florida Current transport and the upper mid-ocean transports (see Sect. 4 for more details). Note that it is an observational estimate of a composite of the main contributions with an unknown residual term that is assumed to be small and barotropic. It does not include other ageostrophic components than the Ekman component. The array has temporally high sampling, i.e. 12 hourly but does not have spatially high sampling across the latitude and depths. The observational timeseries are 5 yr long, from April 2004 to March 2009. We average the 12-hourly measurements (10-day low-pass filtered) to produce 5-daily data for comparison to the 5-daily model data. The 5-daily data has a standard deviation only 3.2 % less than that of the 12-hourly data.

## 3 Comparison of simulated and observed variability

We calculate the timeseries of the 5-daily Atlantic meridional overturning transport at about 26° N in models and measurements. The overturning transport  $T_{\text{over}}$  at a given latitude  $y$  and time  $t$  is the zonal and vertical integral of the meridional velocity  $v$

$$T_{\text{over}}(y, t) = \int_x \int_z^0 v(x, y, z', t) dz' dx \quad (1)$$

where  $x$  and  $z$  are the zonal and vertical axes respectively and the zonal integral is across the whole width of the Atlantic basin. We take the depth integral from the surface ( $z' = 0$ ) to a depth of  $z' \simeq 1000$  m (or to the bottom at longitudes where the ocean is shallower than  $z$ ), to include all of the northward branch of the AMOC. The precise latitude and depth for evaluating  $T_{\text{over}}$  are chosen for each model to coincide with a boundary between model cells in each direction and are shown in Table 1. By construction, the value of  $T_{\text{over}}$  is identical with the meridional overturning streamfunction at the given latitude and depth. At about 26° N, all models have a long-term mean strength in the range 16–21 Sv, within 10 % of the observed 18.6 Sv (Table 1). HiGEM has the smallest time-mean and FAMOUS the largest.

Substantial variability on short time scales is evident in models as well as in observations in the timeseries for a single year (Fig. 1a), shown as an illustration. Calculating the

5-daily standard deviation at 26° N for this single year gives 3–5 Sv for the observations and all the models except FRUGAL and GENIE (Table 1). This is remarkable, given the wide range of complexity of the models, and it is interesting that the magnitude of simulated variability does not depend on model resolution. GENIE and FRUGAL have no high-frequency variability. These models use the UVic atmosphere model which does not have internal dynamics capable of generating variability. In both the models, ocean is forced by prescribed annual wind-stress climatology. It is likely that in the other models the atmosphere provides most of the ocean variability (Gregory et al., 2005). Indeed, when the GENIE ocean is coupled to a dynamical atmosphere (Lenton et al., 2007), notable interannual AMOC variability is generated.

A single year is not representative of climatological statistics, so we calculate the mean annual cycle from the 10 individual years for each model and the 5 yr of observations (Fig. 1b). The high-frequency variability is thereby reduced, but still notable; the 5-daily standard deviation remains similar across most models and is slightly larger in observations (Table 1). Part of the variability comes from the annual cycle. The observations show a maximum in autumn and a minimum in spring whereas the models show a range of seasonal behaviour (Fig. 2).

The variance spectra of the time series (Fig. 1c) show that the annual cycle is the dominant period in both models and observations. In all the models, its variance is within a factor of two of that of observations. At the highest frequencies, however, all the models except CHIME have greater variance than observations, by up to an order of magnitude, with no systematic dependence on model resolution. FAMOUS shows particularly large variance in shorter periods. CHIME shows least variance both for the annual cycle and at high frequencies. Since it uses the same atmosphere model as HadCM3, this difference must be due to the ocean model in some way. Oscillations of less than 40-day period are significant in all the models (except FRUGAL and GENIE) and observations.

The results we describe in this section and the next are based on the 5 yr of observations available so far and 10 yr of model data. We reach the same conclusions if we use either the first 5 yr of the model data or the last 5 yr i.e. the same length as the observations, instead of ten years. The 5-daily standard deviation of each year of the simulations and observations are shown in Fig. 3.

## 4 Dynamical decomposition of the transport

In order to identify the physical sources of variability in the simulated overturning, a dynamical decomposition of the transport is carried out on the 5-daily timeseries. Previous modelling studies (Lee and Marotzke, 1998; Hirschi et al., 2003; Sime et al., 2006; Baehr et al., 2009) suggest

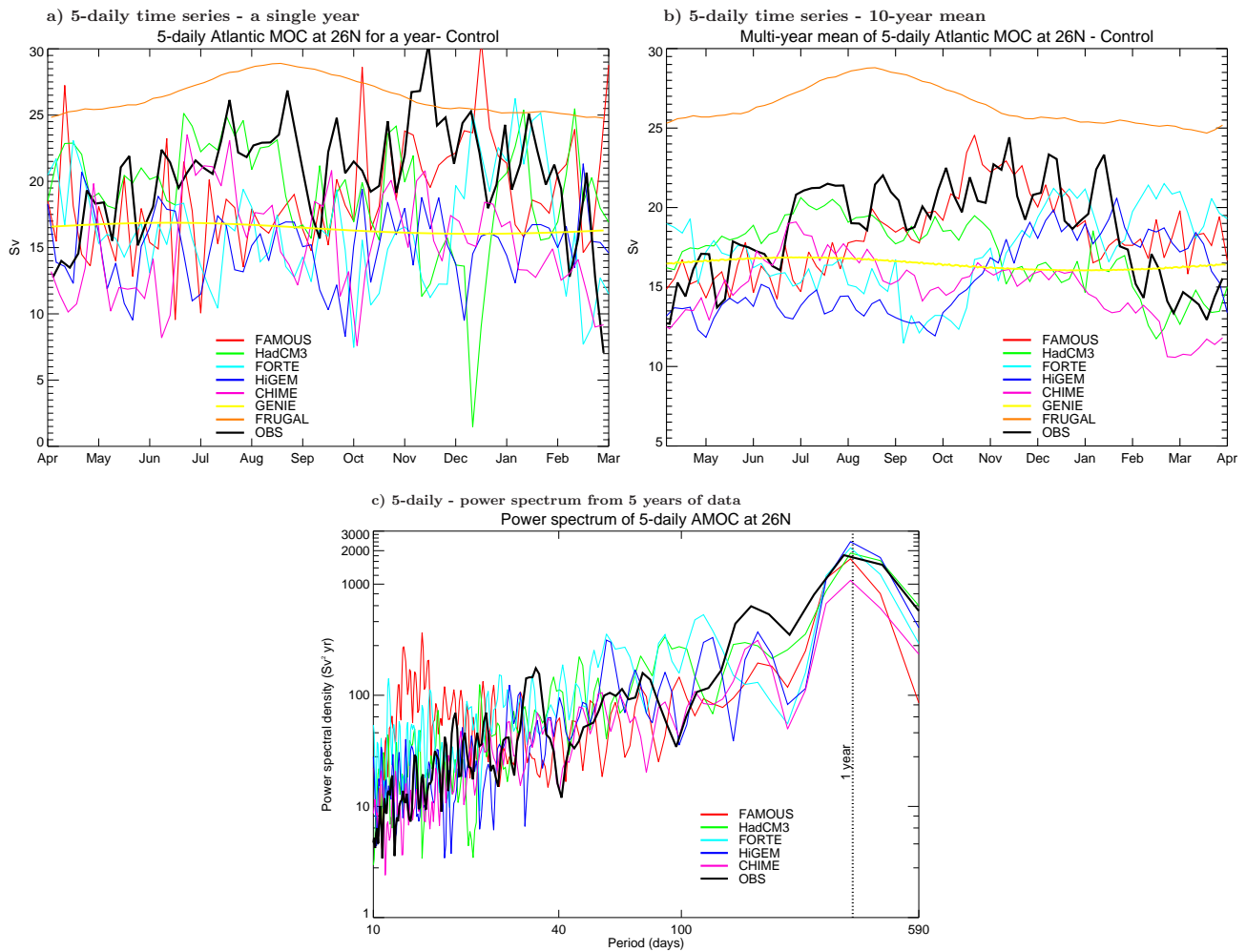


**Fig. 1.** Atlantic MOC ( $T_{over}$ ) at  $26^{\circ}$  N (a) 5-daily time series – for a single year (the second year of the model integrations and observations) (b) 5-daily time series – 10-yr mean in models and 5-yr mean in observations (The FRUGAL transport is calculated along a curvilinear gridline which is near  $26^{\circ}$  N. For GENIE, time-step data is plotted; its ocean time-step is 3.65 days) and (c) 5-daily – power spectrum (Note the logarithmic scale on the y-axis. Oscillations of less than 40-day period are significant in observations and in all the models, except FRUGAL and GENIE).

various ways of decomposing the transport. Cunningham et al. (2007) obtain the observational  $T_{over}$  from Ekman, Florida Current and upper mid-ocean components, of the RAPID/MOCHA array. The Ekman component is physically distinguished; it exists within the upper tens of metres which are affected by the windstress and the vertical shear it causes. The Florida Current component is geographically distinguished; it is the integral of flow at all depths passing through the narrow channel between Florida and the Bahamas, within which there is a specific monitoring system. The channel is 800 m deep and the flow through it is entirely counted in the northward branch of the AMOC. The upper mid-ocean component is the geostrophic meridional flow above 1100 m through the  $26.5^{\circ}$  N section across the Atlantic from the Bahamas to Africa.

Florida and the Bahamas are not represented with realistic geography, or at all, in the models. Hence we cannot meaningfully calculate the Florida Straits transport, and instead we carry out the decomposition slightly further north, at around  $29^{\circ}$  N, between the coasts of America and Africa. (At the end of this section, we evaluate the western boundary current in the models.) Again, the precise latitude is model-dependent, and the same depth is used as for  $26^{\circ}$  N (Table 1). Our decomposition of  $T_{over}$  is physically based, consistent with the model formulations, into Ekman, geostrophic, viscous and advective components.

Consider the equation of motion. The zonal acceleration is given as

$$\frac{Du}{Dt} = \mathbf{u} \cdot \nabla \mathbf{u} + \frac{\partial \mathbf{u}}{\partial t} = -\frac{1}{\rho} \frac{\partial P}{\partial x} + fv + F_v + F_h \quad (2)$$

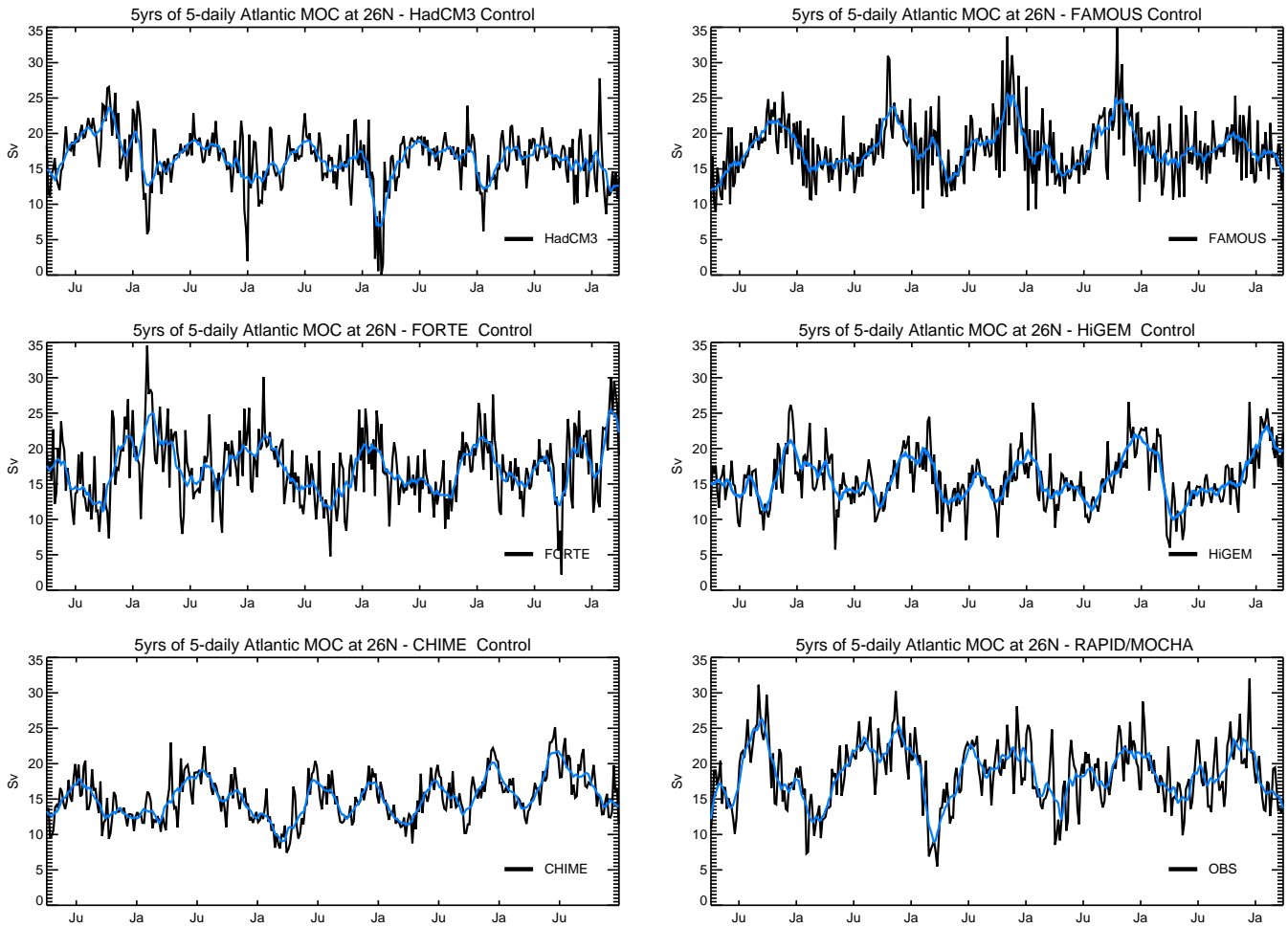


**Fig. 2.** 5-yr timeseries of 5-daily Atlantic MOC ( $T_{\text{over}}$ ) at  $26^\circ$  N in observations and in the RAPID-AOGCMs. (Data with a 45-day moving average is shown in blue.) Other RAPID-models, GENIE and FRUGAL with simple atmospheric components, have little interannual variability. The last 5 yr of the 10 yr of data from each AOGCM is shown here.

where  $\mathbf{u}$  is the 3-D velocity and  $u$  its eastward component,  $\partial P/\partial x$  is the zonal pressure gradient,  $f$  is the Coriolis parameter,  $F_v = \kappa \partial^2 u/\partial z^2$  is the vertical momentum diffusion term with  $\kappa$  the coefficient of vertical viscosity,  $F_h = \eta_{\text{Lap}} \nabla_H^2 u$  and/or  $F_h = \eta_{\text{bi}} \nabla_H^4 u$  (according to model formulation) is the horizontal momentum diffusion term with  $\eta_{\text{Lap}}$  and  $\eta_{\text{bi}}$  being the coefficients of horizontal viscosity, and  $\rho$  is the Boussinesq reference density. We rearrange Eq. (2) and integrate it over depth and longitude across the Atlantic as

$$\int \int_z^0 v dz' dx = \frac{1}{f} \int \int_z^0 \left( \frac{1}{\rho} \frac{\partial P}{\partial x} - F_v - F_h + \mathbf{u} \cdot \nabla \mathbf{u} + \frac{\partial u}{\partial t} \right) dz' dx \quad (3)$$

Thus we treat the total transport on the LHS as a sum of the terms on the RHS as follows.

The geostrophic transport ( $T_{\text{geo}}$ ) is the term due to  $\partial P/\partial x$  and consists of two parts: the internal part ( $T_{\text{int}}$ ), which is due to the pressure gradient  $\partial P_\rho/\partial x$  caused by zonal density gradients, and the external part ( $T_{\text{ext}}$ ), which is due to the sea surface slope  $\partial h/\partial x$  in models with a free surface (HiGEM, FORTE) or to the rigid lid pressure gradient  $\partial P_s/\partial x$  in rigid lid models (HadCM3, FAMOUS and GENIE), where effectively  $P_s = h\rho g$ . Thus

$$\begin{aligned} T_{\text{geo}} &= T_{\text{ext}} + T_{\text{int}}, \\ T_{\text{int}} &= \frac{1}{\rho f} \int \int_z^0 \frac{\partial P_\rho}{\partial x} dz' dx, \\ T_{\text{ext}} &= \frac{1}{\rho f} \int \int_z^0 \frac{\partial P_s}{\partial x} dz' dx \end{aligned} \quad (4)$$

The vertical momentum diffusion  $\kappa \partial^2 u/\partial z^2$  is the vertical derivative of the diffusive vertical momentum flux  $\kappa \partial u/\partial z$ . Integrated over the upper ocean, this equals the surface momentum flux i.e. the zonal wind stress  $\tau_x$ , which

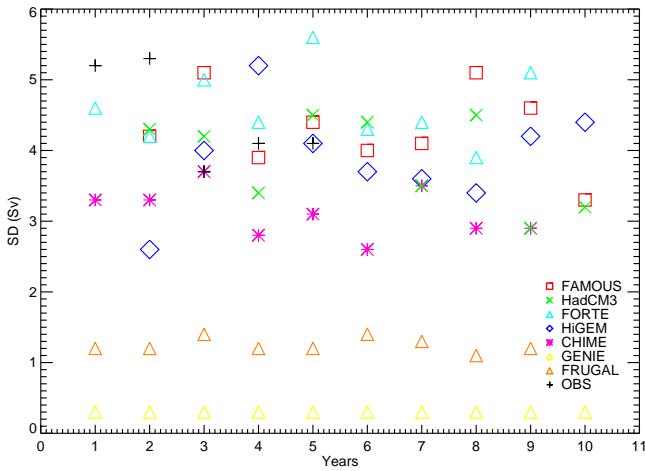


**Fig. 3.** Standard deviation of the 5-daily Atlantic MOC ( $T_{over}$ ) at  $26^\circ$  N for each year of simulations and observations. (Since the observational timeseries starts in April, the SD is calculated from April to March and some models are missing a year because of wanting to start all the years in April.)

is all absorbed in the Ekman layer. The bottom boundary layer is far below, and the bottom stress is identically zero in HadCM3 and FAMOUS, which have a free-slip bottom boundary condition, and is negligible in HiGEM and FORTE. GENIE has no bottom boundary layer or explicit bottom stress. Hence there is no contribution from bottom stress to the Ekman transport

$$T_{Ek} = -\frac{1}{\rho f} \int \tau_x dx. \quad (5)$$

The ageostrophic transport due to the horizontal momentum diffusion i.e. horizontal viscosity is

$$T_{vis} = -\frac{1}{f} \int \int_z^0 \eta_{Lap} \nabla_H^2 u dz' dx \quad \text{and/or} \\ T_{vis} = -\frac{1}{f} \int \int_z^0 \eta_{bi} \nabla_H^4 u dz' dx \quad (6)$$

The horizontal diffusion terms are Laplacian ( $\nabla_H^2 u$ ) and/or biharmonic ( $\nabla_H^4 u$ ) formulations with different coefficient of viscosity in each model. In theory these viscous terms represent the horizontal momentum flux due to unresolved eddies, although in practice horizontal viscosity is increased to ensure model dynamical stability. The viscous term can locally be of either sign, since its effect is to transport momentum. Globally, it must sum to zero for momentum, but is a positive definite sink of kinetic energy.

The advective transport ( $T_{adv}$ ) due to the non-linear advective term  $\mathbf{u} \cdot \nabla u$  is

$$T_{adv} = \frac{1}{f} \int \int_z^0 \mathbf{u} \cdot \nabla u dz' dx \quad (7)$$

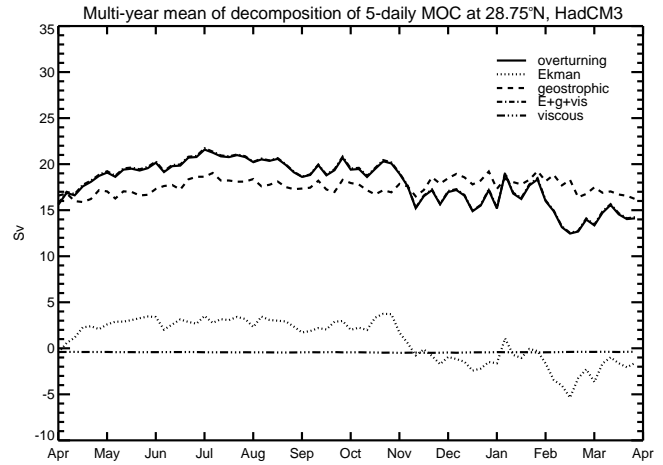


**Fig. 4.** Decomposition of 5-daily Atlantic MOC ( $T_{over}$ ) into physical components at about  $29^\circ$  N in HadCM3. The sum  $E + g + vis$  (dash-dotted) is almost coincident with the total overturning (solid).

where the momentum flux due to resolved eddies would appear. This term is absent in GENIE by construction.

In HadCM3, FAMOUS and HiGEM we can calculate all the components. Any residual is due to acceleration  $\partial u / \partial t$ . The residual due to the local acceleration is negligibly small and is ignored in all models, so

$$T_{over} = T_{geo} + T_{Ek} + T_{vis} + T_{adv} \quad (8)$$

As an example, this decomposition is shown for HadCM3 in Fig. 4. In GENIE, we calculate  $T_{over}$ ,  $T_{Ek}$  and  $T_{vis}$ , and infer  $T_{geo}$  as a residual. This model uses an annual climatology of windstress as a constant term, so  $T_{Ek}$  does not contribute to variability. In FORTE, we calculate  $T_{over}$ ,  $T_{Ek}$  and  $T_{vis}$  due to the Laplacian diffusion term, and infer  $T_{geo}$  as the residual. This means that the biharmonic diffusion term is included in  $T_{geo}$ . This term is implicit in the model (Webb et al., 1998) and could not be calculated offline. It is relatively large and it is unclear how to interpret it physically. The components of transport could not be computed for FRUGAL and CHIME.

The mean and 5-day variability of the components of observed and simulated transports are shown in Table 1. The observed geostrophic transport is the sum of the mid-ocean transport and Florida current transport. In the mean, the geostrophic term is largest in all cases. The Ekman term is relatively small and positive, and the viscous term even smaller and negative, except in GENIE, in which the viscous (actually frictional) term is larger than in other models and the signs of these two terms are the other way round.

As discussed above, the largest part of the variability is the mean annual cycle. The two main sources of this variability are  $T_{Ek}$  (Fig. 5a) and  $T_{geo}$  (Fig. 5b) in the models, as in observations (Cunningham et al., 2007). However,  $T_{geo}$  variability is smaller than  $T_{Ek}$  variability in models whereas in observations the reverse is true (Table 1). It is evident in Fig. 4 that

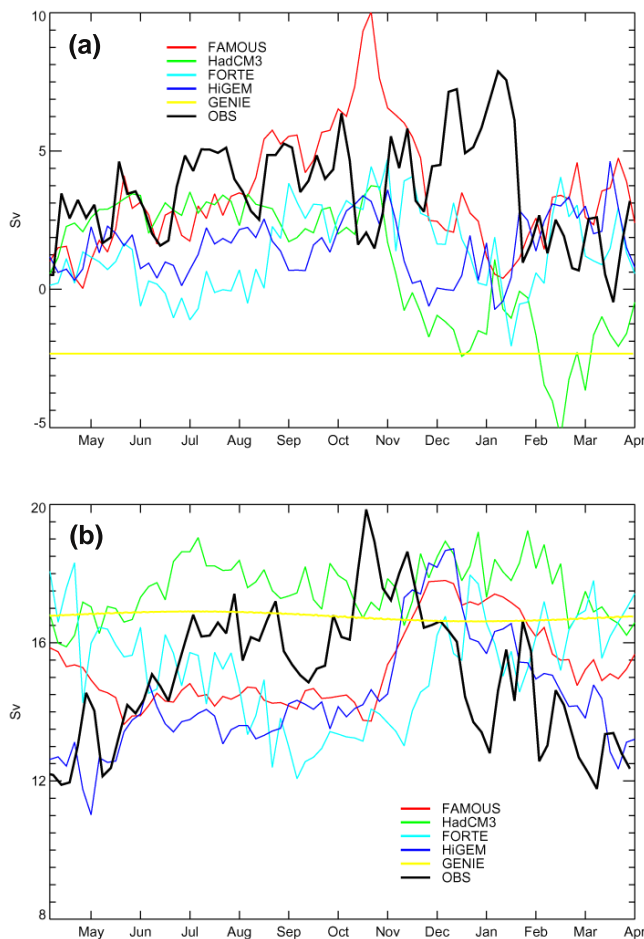


**Fig. 5.** Annual cycle of 5-daily Atlantic MOC ( $T_{\text{Over}}$ ) components at about  $29^\circ\text{N}$  – (a) Ekman component ( $T_{\text{Ek}}$ ) and (b) Geostrophic component ( $T_{\text{geo}}$ ).

the Ekman term dominates the annual cycle in HadCM3, for example.

We find that  $T_{\text{geo}}$  variability tends to be underestimated in models as compared to observations. In the observations, the variability is found to be due to the effect of the seasonal momentum flux on the eastern boundary density (Chidichimo et al., 2010; Kanzow et al., 2010). This suggests that models might underestimate the variability of the pressure anomaly along the eastern/western boundaries, possibly as the result of underestimating the adiabatic upwelling/downwelling processes driven by alongshore wind-stress due to the coarse resolution which spreads the effect over one grid box instead of a more confined area in reality. As the geostrophic seasonal cycle is mainly driven by surface fluxes, unrealism in either the surface fluxes or the vertical mixing caused by the surface fluxes could also be a cause of underestimated variability in models. In eddy-permitting HiGEM, the geostrophic seasonal cycle has more variability than in HadCM3 (Fig. 5c), and dominates the shape of the annual

cycle, as in observations. This is true also of FORTE, but in that case the “geostrophic” term actually includes a large residual due to the biharmonic diffusion (as noted above).

As in the observed variability (Kanzow et al., 2007), the external  $T_{\text{ext}}$  and internal  $T_{\text{int}}$  components of  $T_{\text{geo}}$  in the upper 1000 m strongly anticorrelate in most models (Table 1) since by construction,  $T_{\text{geo}}(z, t) = T_{\text{int}}(z, t) + T_{\text{ext}}(z, t)$ , where  $z$  is a suitably chosen depth, so that  $dT_{\text{int}}/dt = -dT_{\text{ext}}/dt + dT_{\text{geo}}/dt$ . Indeed, this expression shows that a strong anticorrelation between  $T_{\text{int}}$  and  $T_{\text{ext}}$  should be observed whenever the fluctuations in  $T_{\text{geo}}$  become small relative to that of  $T_{\text{ext}}$  and  $T_{\text{int}}$ , mathematically when  $|dT_{\text{geo}}/dt| \ll |dT_{\text{int}}/dt|$ , which when it occurs expresses deep compensation. According to classical theories describing the spin-up of a stratified ocean in response to change in wind forcing, e.g. Anderson and Killworth (1977), Anderson and Corry (1985), the physical mechanism for such a deep compensation is speculated to be associated with the baroclinic adjustment by oceanic Rossby waves, which is usually found to compensate the barotropic response (that usually characterizes the initial stages of the adjustment to a change in the wind forcing) in the deeper layers. Note that an external component,  $T_{\text{ext}}$ , is not considered in Cunningham et al. (2007) and Kanzow et al. (2010); instead the compensation term for the mass-conservation plays this role, in effect.

Variability due to the viscous term  $T_{\text{vis}}$  is small but not quite negligible. This term is not calculated for the observational array, because it represents the effect of unresolved motion and, by definition, any quantity measured by the array has been “resolved” by it. The analogue of this term would be any contribution to  $T_{\text{over}}$  from ageostrophic motion; the observational estimate assumes that the motion is geostrophic or Ekman, as it has to do because the current is not directly measured at all, except in the Florida Straits and near the western boundary. Consequently the array cannot measure the ageostrophic contribution due to the advective term, which is found to be negligible in HadCM3, FAMOUS and FORTE. However, in eddy-permitting HiGEM,  $T_{\text{adv}}$  makes a considerable contribution, of about 2 % of the total mean transport and 17 % of the total transport variability. It might therefore be a significant omission from the monitoring system.

Our physical decomposition does not include an explicit Gulf Stream component, which in reality passes through the Florida Straits. As discussed above, this is not geographically resolved in all the models, but we can estimate the northward western boundary current transport ( $T_{\text{GS}}$ ) in the models, defined geographically. To be consistent with the latitude of our decomposition and to quantify its contribution to the geostrophic transport variability, the  $T_{\text{GS}}$  estimate is also done at about  $29^\circ\text{N}$ .

The  $T_{\text{GS}}$  at a given latitude  $y$  and time  $t$  is the zonal and vertical integral of the meridional velocity  $v$  between the western boundary,  $x_w$ , and longitude,  $x_e$ , and between the surface and  $z$ , the depth of the maximum of AMOC at about

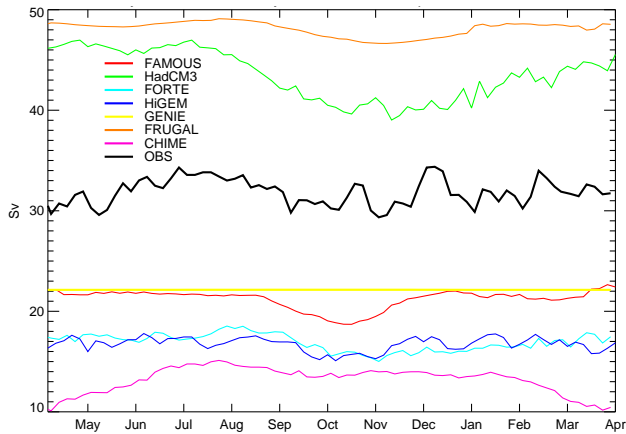


**Fig. 6.** Annual cycle of 5-daily western boundary current transport ( $T_{GS}$ ) at about  $29^\circ$  N calculated geographically (see Sect. 4 for details).

$29^\circ$  N. The exact depth and latitude for each model are the same as stated in Table 1.

$$T_{GS}(y, t) = \int_{xw}^{xe} \int_z^0 v(x', y, z', t) dz' dx' \quad (9)$$

The eastern bound,  $x_e$ , is chosen for each model separately as the longitude which gives the maximum  $T_{GS}$  in the long-term mean.

The  $T_{GS}$  component in all the RAPID-models are shown in Fig. 6. HadCM3 and FRUGAL overestimate the time-mean  $T_{GS}$  while all other models underestimate (Table 1). There is a much wider model spread in  $T_{GS}$  than in  $T_{over}$ , pointing to large differences in the simulations of the wind-driven gyre circulation. While the observed variability is 3 Sv, the simulated variability is mostly in the 1–2 Sv range except for HadCM3 with the greatest value and GENIE the least. Apart from CHIME and GENIE, most models show minimum transport in autumn. The seasonal cycle of the Florida Straits transport using longer observations (Atkinson et al., 2010) shows a summer maximum and a winter minimum. The observed seasonal cycle using the monthly means of first 4 yr of RAPID/MOCHA observations is also shown in Kan-zow et al. (2010).

## 5 Meridional coherence of transport and its components

The canonical picture of a meridionally coherent overturning transport is contradicted by recent studies such as Bingham et al. (2007), Willis (2010) and Lozier et al. (2010). Bingham et al. (2007) found in two different ocean GCMs that the AMOC variability south of  $40^\circ$  N is dominated by high-frequency variability whereas north of  $40^\circ$  N it is dominated by decadal variability. Based on satellite and float observations of sea surface height, temperature, salinity and veloc-

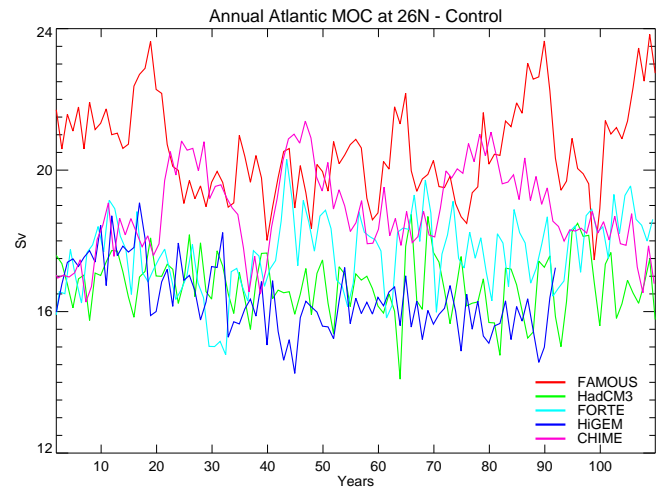


**Fig. 7.** Annual time series of the Atlantic MOC ( $T_{over}$ ) at  $26^\circ$  N (HiGEM data is only 90 yr long after the spin-up time).

ity, Willis (2010) estimated the AMOC at  $41^\circ$  N which has smaller seasonal and interannual variability than at lower latitudes. Using both hydrographic observations and a numerical model, Lozier et al. (2010) detected gyre-specific decadal changes in the AMOC.

In Fig. 7 we show the annual timeseries of  $T_{over}$  at  $26^\circ$  N. The observed timeseries is not yet long enough to assess variability on multiannual timescales. FAMOUS and CHIME have greater long-period variability than other models.

A commonly used AMOC index from AOGCM results is  $M_{max}$ , the maximum of the overturning streamfunction, wherever it occurs, within a range of latitude and depth in the Atlantic, rather than at fixed latitude and depth. The RAPID/MOCHA array is intended to monitor the AMOC, by measuring the circulation at only one latitude. In the model results we can investigate how well  $M_{max}$  and  $T_{over}$  at  $26^\circ$  N represent  $T_{over}$  at other latitudes, in order to test the conventional assumption that the temporal variability of the circulation is coherent throughout the basin. GENIE is omitted from this analysis because it has no high-frequency or interannual variability, and CHIME and FRUGAL because all required timeseries are not available.

Calculated from 5-day means in the RAPID-models, the time-mean  $M_{max}$  is larger than the transport at  $26^\circ$  N, as it must be by construction, but the variability of  $M_{max}$  is generally less (Table 1). In annual means, however, the two timeseries have similar standard deviations. We have evaluated the same statistics from the AOGCMs of the Coupled Model Intercomparison Project Phase 3 (CMIP3), finding that in 16 out of 20 of them the annual standard deviation is similar in  $M_{max}$  and at  $26^\circ$  N (Table 2) (“similar” when the difference between 2 standard deviations is less than 0.5 Sv); the exceptions are GISS-ER, GISS-AOM, INM-CM3.0 and IAP-FGOALS1.0g. That suggests greater coherence across

**Table 2.** Comparison of standard deviations (in Sv) of Atlantic MOC ( $T_{\text{over}}$ ) at 26° N, 50° N and of the maximum of Atlantic MOC,  $M_{\text{max}}$ , and their correlations in the CMIP3 models. Linear or quadratic trend is removed for unsteady runs before the calculation. The lag between  $T_{\text{over}}$  at 26° N and 50° N is shown which gives the largest correlation of their timeseries. The lag is negative when  $T_{\text{over}}$  26° N lags.

Model	SD $M_{\text{max}}$	SD $T_{\text{over}}$ 26° N	Corr ( $T_{\text{over}}$ 26° N, $M_{\text{max}}$ )	SD $T_{\text{over}}$ 50° N	Corr ( $T_{\text{over}}$ 26° N, $T_{\text{over}}$ 50° N)	Lag (years)	Lagged Corr. ( $T_{\text{over}}$ 26° N, $T_{\text{over}}$ 50° N)
CSIRO-Mk3.0	1.8	1.6	0.85	1.6	0.53	-1	0.70
CNRM-CM3	1.8	2.1	0.20	1.7	0.05	-2	0.41
CCCMA-CGCM3.1(T63)	0.72	0.71	0.85	0.67	0.11	-1	0.51
CCCMA-CGCM3.1(T47)	0.50	0.63	0.09	0.65	-0.14	-2	0.39
BCCR-BCM2-0	0.93	0.91	0.61	0.82	-0.02	-2	0.25
GISS-ER	2.7	0.97	0.06	2	0.35	-1	0.48
GISS-AOM	7.2	1.5	0.01	2.0	0.19	-3	0.44
GFDL-CM2.1	1.3	1.2	0.39	1.1	-0.01	-5	0.46
GFDL-CM2.0	1.1	1.1	0.38	1.1	0.12	-2	0.51
CSIRO-Mk3.5	1.2	1.0	0.88	1.4	0.52	-1	0.72
MIROC3.2(hires)	0.8	1.0	0.16	0.82	0.02	-1	0.28
INM-CM3.0	2.9	3.4	0.47	1.7	0.07	-2	0.52
INGV-ECHAM4	1.6	1.9	0.61	1.5	0.09	-3	0.58
IAP-FGOALS1.0g	2.3	0.49	0.09	0.43	-0.26	10	-0.02
NCAR-CCSM3.0	1.8	1.2	0.88	1.1	0.24	-2	0.45
MRI-CGCM2.3.2a	0.71	0.73	0.53	0.97	-0.23	-1	0.34
MIUB-ECHOG	1.3	1.0	0.35	1.2	0.23	-4	0.53
MIROC3.2(medres)	0.72	0.64	0.67	0.69	0.07	-2	0.44
UKMO-HadGEM1	1.0	1.0	0.68	0.77	0.05	-1	0.21
UKMO-HadCM3	1.7	1.8	0.54	1.2	0.05	1	0.21

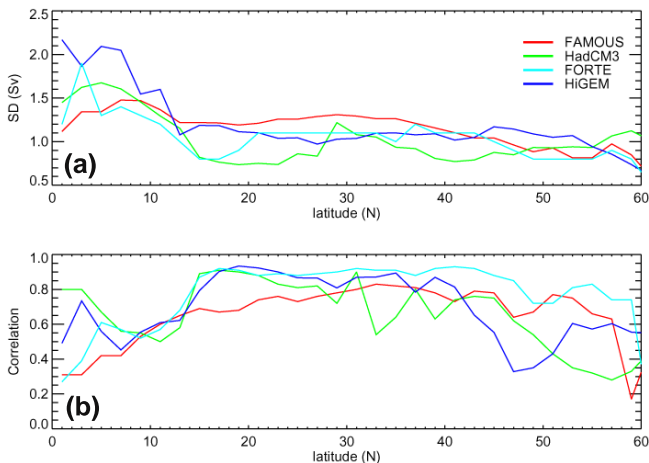


**Fig. 8.** Zonal profile of (a) annual ocean meridional overturning transport ( $T_{\text{over}}$ ) variability (Sv) and (b) correlation of annual  $T_{\text{over}}$  and ocean meridional heat transport in the North Atlantic.

latitudes at longer time periods. However, only ten of the CMIP3 models and three of the RAPID-models have high correlation (exceeding 0.5) between the two timeseries. This is likely to be because there is a time lag between 26° N and the latitudes of  $M_{\text{max}}$ . Figure 8a shows the annual standard deviation of total transport as a function of latitude. No model has a well-defined maximum, but there is generally more variability in the tropics, diminishing towards

higher latitudes. This low-latitude variability found in the AMOC and also in the AOHT is wind-induced (Klinger and Marotzke, 2000; Jayne and Marotzke, 2001; Marsh et al., 2009). In a 1000-yr-long GFDL-CM2.1 control integration (Zhang, 2010), the maximum of interannual variability is found at about 35° N.

Next, we calculate the temporal correlation between different latitudes of timeseries of annual and 5-daily volume transports and their Ekman and geostrophic components, in HadCM3, FAMOUS, FORTE and HiGEM. Positive correlations are found between neighbouring latitudes in all time-series, diminishing with increasing separation (e.g. for annual timeseries in HiGEM, Fig. 9). Anticorrelation is found for widely spaced latitudes in the Ekman component. Since this component is wind-forced, the anticorrelation must indicate opposing signs of zonal windstress, occurring on opposite sides of the anomalies in atmospheric pressure and circulation that produce the windstress anomalies, in particular associated with the moving front between subpolar and subtropical gyres. It is notable that the anticorrelation is found for both 5-daily (figure not shown) and annual data, even more pronounced in the former.

We define the “correlation length” as a function of latitude  $y$  to be the width of the range of latitudes whose timeseries have a temporal correlation exceeding 0.5 with the timeseries at latitude  $y$ . Within 15–60° N, the correlation lengths are typically 20–40° in the annual timeseries (see Table 1 for 26° N and Fig. 9 for HiGEM). Correlation lengths are greater

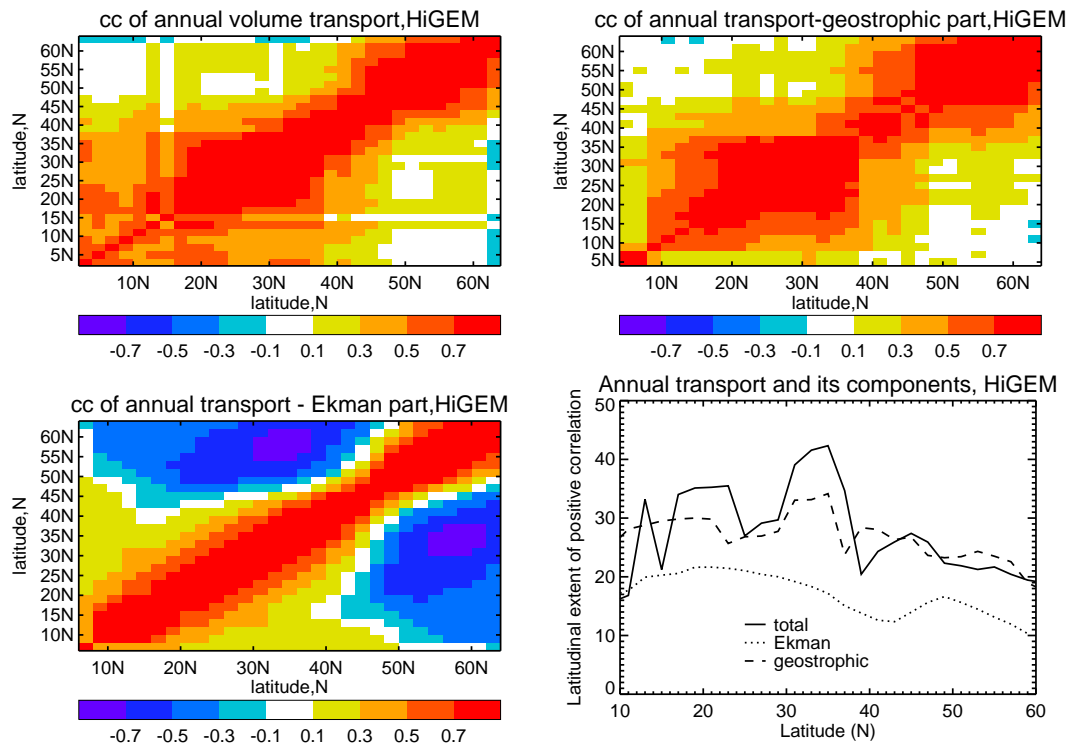


**Fig. 9.** Cross-correlation of ocean meridional overturning transport,  $T_{\text{over}}$  and its physical components, between latitudes in the North Atlantic in HiGEM: annual  $T_{\text{over}}$  (top left), geostrophic,  $T_{\text{geo}}$  (top right), Ekman,  $T_{\text{ek}}$  (bottom left) and their meridional correlation length (bottom right). Correlation length ( $^{\circ}\text{lat}$ ) as a function of latitude  $y$  is defined as the width of the range of latitudes whose timeseries which have a temporal correlation exceeding 0.5 with the timeseries at latitude  $y$ .

for the annual total and the geostrophic components than for the Ekman. They are also greater for annual total transports than for 5-daily total transports, due to the greater coherence of the annual geostrophic component. Shaffrey and Sutton (2004, their Fig. 1d) and Bingham et al. (2007, their Fig. 2) also showed long-range coherence of annual total transport for HadCM3 and OCCAM models. The lowest correlation length is found at about  $40^{\circ}\text{N}$ .

Given the typical correlation length, we conclude that the transport measured by the RAPID/MOCHA array is likely to have a correlation of less than 0.5 with the AMOC strength in the mid-to-high latitude Atlantic, where it has its greatest importance to climate variability (see Sect. 6). In the CMIP3 data, we test this by correlating timeseries of  $T_{\text{over}}$  at  $26^{\circ}\text{N}$  and  $50^{\circ}\text{N}$ ; only two models have a coefficient exceeding 0.5. Correlation is increased somewhat by including lags of a few years, but still does not exceed 0.5 in most cases. In models where there is a lag, variability of  $T_{\text{over}}$  at  $50^{\circ}\text{N}$  precedes  $26^{\circ}\text{N}$ , indicating that the forcing of the large-scale geostrophic variability comes from the north. A similar relation between AMOC at  $26^{\circ}\text{N}$  and  $50^{\circ}\text{N}$  with a time lag of 4 yr is found in GFDL-CM2.1 (Zhang, 2010). The mechanism behind this time lag is caused by changes in deep water formation occurring at the high latitudes and initiating Kelvin waves, which propagate southward along

the western boundary. These coastally trapped Kelvin waves are manifest as transport anomalies at each latitude as they propagate from the north to the equator, eastward along the equator to the eastern boundary, and then poleward along the eastern boundaries (Johnson and Marshall, 2002). Recently, Zhang (2010), using a coupled AOGCM which represents the interior pathways of North Atlantic Deep Water in the mid-latitudes as observed by Bower et al. (2009), found that AMOC variations propagate in an advective manner in the mid-latitudes and at the speed of Kelvin waves in the subtropics along the western boundary.

## 6 Relation of northward volume transport to heat transport

The climatic relevance of the AMOC arises from its association with the northward heat transport. The seasonal to interannual meridional Atlantic Ocean heat transport (AOHT) variability in tropics and subtropics is associated with the wind-driven Ekman transport (Klinger and Marotzke, 2000; Jayne and Marotzke, 2001; Marsh et al., 2009). We assess the relationship between AMOC and AOHT by correlating the annual-mean time series of the AMOC to that of the AOHT at different latitudes (Fig. 10) in the North

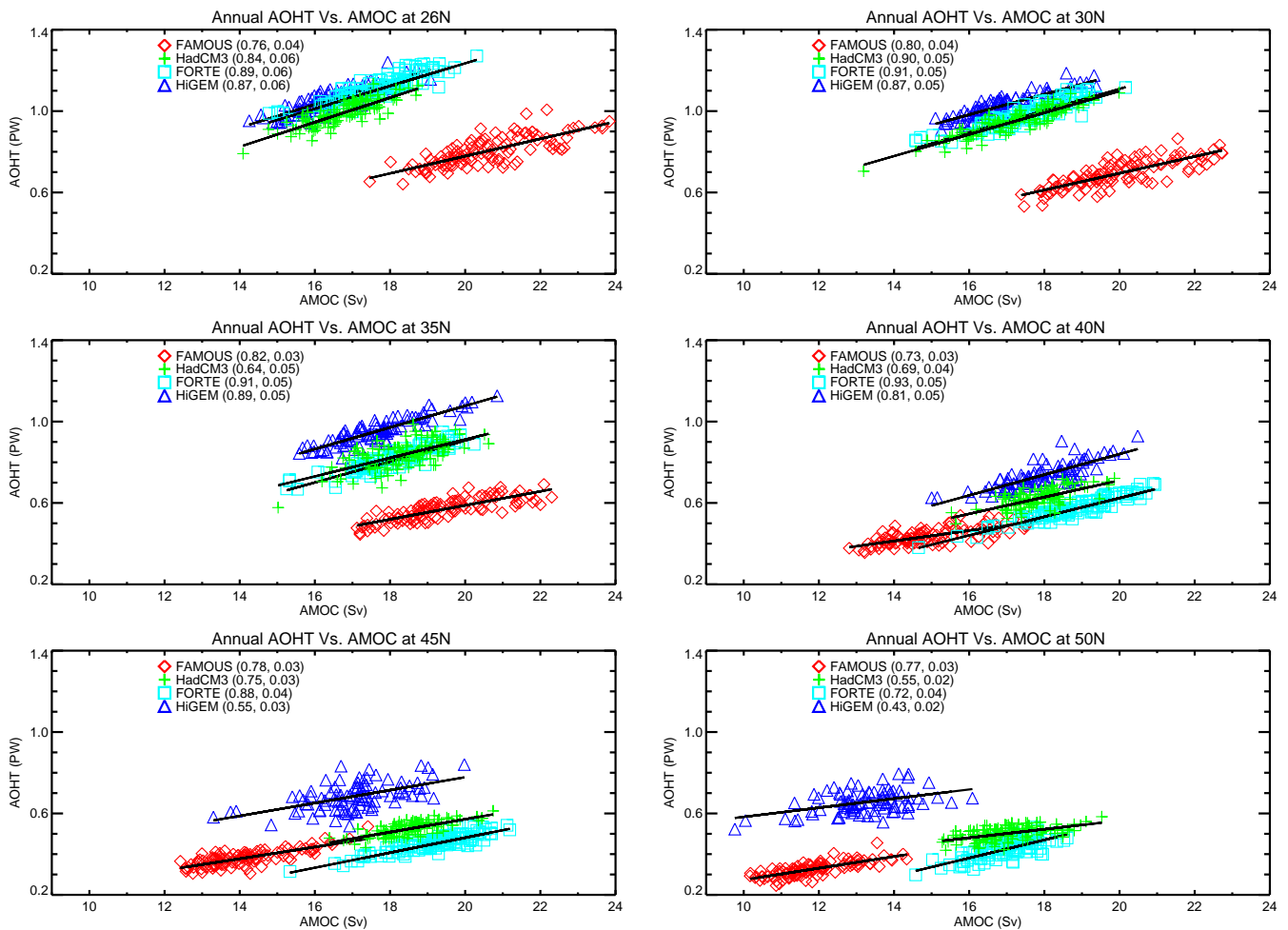


**Fig. 10.** Scatter plot of annual-mean ocean meridional overturning transport,  $T_{\text{over}}$  (Sv) and ocean meridional heat transport (PW) at various latitudes in the North Atlantic in different models. The correlation coefficients and slopes of the regression are given in brackets.

Atlantic. This analysis can only be done for HadCM3, FAMOUS, FORTE, HiGEM and partly for CHIME. (AOHT is unavailable for other RAPID models and most of the CMIP3 models.) As expected, the time-mean heat transport is maximum around 10–30° N, where it is about 1 PW (Fig. 11a, Table 1) in models. Compared to the observational estimate of Ganachaud and Wunsch (2003), HiGEM and FORTE values are within the error bars of 2 of the 3 North Atlantic latitudes, while HadCM3 and CHIME are closer to the estimate around 50° N. FAMOUS heat transports are generally underestimated. Like  $T_{\text{over}}$ , the AOHT does not have a well-defined maximum in variability as a function of latitude (Fig. 11b). At 35° S in the Atlantic, Dong et al. (2009) found that much of the observed northward heat transport variability is associated with the overturning component and the two are significantly correlated. Johns et al. (2011) estimated that half of the array-AOHT variability at 26° N is due to the Ekman component and the other half by the geostrophic component.

Though the volume and heat transport variations in the RAPID-models do not have a similar zonal profile, in general a good degree of temporal correlation is found between them at all latitudes from 15° N to 45° N (Fig. 10, 8b, Table 1 for 26° N). Towards higher latitudes, the contribution due to the overturning decreases. The slopes of the regression are fairly similar between 26–45° N, indicating the positive volume-heat transport relationship at these latitudes. However, since the AMOC at 26° N and 50° N are not strongly correlated (Sect. 5), we expect that AOHT at 50° N, in the latitudes of the northern Europe, is not strongly correlated with the AMOC at 26° N. Indeed this is the case in HadCM3, FAMOUS, FORTE, CHIME and HiGEM (Table 1). The high-latitude AMOC index is more important for climate variability because it is supposed to reflect most directly the rate of deep water formation; this is obscured by wind-driven variability in the AMOC at 26° N.

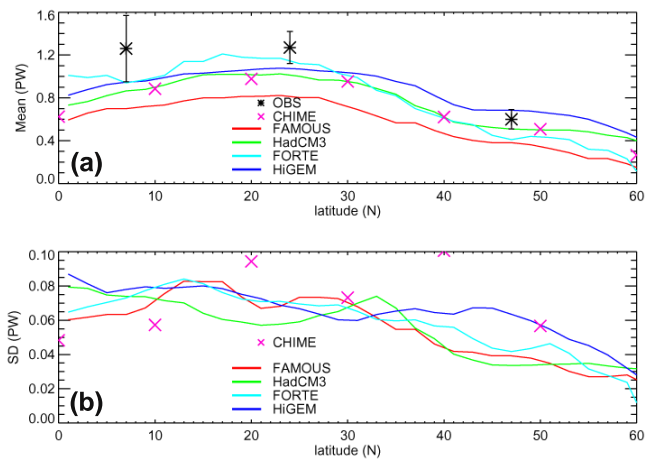


**Fig. 11.** Zonal profile of (a) mean annual ocean meridional heat transport (PW) and (b) variability of annual ocean meridional heat transport in the North Atlantic. The observational estimate of heat transport is from Ganachaud and Wunsch (2003). CHIME data is only available in  $10^\circ$  latitude intervals.

## 7 Summary and discussion

The RAPID/MOCHA array has produced a dataset which permits us to assess model simulations of the AMOC in new ways. We have shown that the 5-daily standard deviation of the AMOC at about  $26^\circ$  N simulated in the RAPID set of coupled climate models is comparable to that of the RAPID/MOCHA observational estimate. This is an evaluation of a property that is unlikely to have been “tuned” during model development, because the observational estimate is new and recent, unlike the time-mean of the AMOC, which is customarily evaluated in models. The standard deviation has contributions from high-frequency variability (timescale of a few days), the annual cycle and interannual variability. The models generally have more high-frequency variability than that estimated from observations, and a similar amplitude of annual cycle, but a spread in simulating the shape of the cycle.

Surprisingly, there is no systematic relation between the model resolution and the magnitude of variability. This contradicts to the general assumption that if the resolution is increased, variability in all timescales will be increased. Wunsch (2008) contended that eddies could possibly dominate the variability of the measured transport, and thereby prevent the detection of a possible trend in too short records, but since recent studies such as Kanzow et al. (2009), it has been increasingly appreciated that eddies would be swept away as coastally-trapped waves upon reaching the western boundaries, leaving only a weak signal in the zonally-integrated volume transport. All the models used in our study are of coarse resolution, except for HiGEM, which is eddy-permitting. The relative insensitivity to model resolution could therefore be due to the fact that none of the models

are able to generate enough eddy variability for this to affect the simulated transport variability substantially. In experiments done with different resolutions of OCCAM OGCM, it is found that the eddy-resolving version produced realistic AMOC variability compared to observations (Marsh et al., 2009; Cunningham and Marsh, 2010).

We have dynamically decomposed the variability at about  $29^\circ$  N (slightly north of the RAPID/MOCHA array in order to avoid complications with model coastlines) into Ekman, geostrophic (i.e. due to pressure and sea-level gradient) and viscous/frictional components. The AMOC at  $29^\circ$  N is predominantly geostrophic, but the Ekman term also contributes to variability. Ekman variability is more important in models than in observations. Other ageostrophic terms are neglected in the observational estimate, but are not negligible in models; in particular, the advection of momentum makes a significant contribution to AMOC variability in HiGEM. Our decomposition into the terms of the model equation of motion gives information about the realism of the simulation of the relevant processes, and we suggest that such a decomposition of the transport would be useful to carry out with other AOGCMs. We have also quantified the western boundary current transport at  $29^\circ$  N, for comparison with the observed Florida Straits transport. The models diverge much further from the observational estimate in the time-mean of the western boundary current than they do with the AMOC, suggesting large differences in the simulation of the wind-driven gyre. As with the geostrophic contribution to the AMOC, the variability of the western boundary current is less in the models than observed.

Though we have not narrowed down the specific mechanisms responsible for the simulated high-frequency variability, our results point out the role of atmosphere in setting it. In models with simple atmospheres, there is little high-frequency variability.

In the RAPID models and in most CMIP3 AOGCMs, the magnitude of interannual variability in the AMOC at  $26^\circ$  N and in the maximum of the AMOC are similar, the latter being a commonly used model index. (The observational dataset as yet is not long enough to assess simulated interannual variability.) We find that interannual variations in Atlantic Ocean heat transport are fairly well correlated at each latitude with the AMOC, confirming its climatic significance and the robustness of this relationship in models. Correlation between different latitudes is fairly long-range, but does not extend over the whole basin (also found by Lozier et al., 2010). Consequently the AMOC at  $26^\circ$  N does not have a high correlation with the AMOC or with heat transport at mid-to-high latitudes. Since the latter has a practical importance, and because this analysis, Zhang (2010) and Hodson and Sutton (2011) all suggest that AMOC variability on multiannual timescales propagates from north to south, it would be useful to monitor the AMOC and AOHT at higher latitudes as well as the latitude of  $26^\circ$  N occupied by the RAPID/MOCHA array.

**Acknowledgements.** This study was supported by the “UK RAPID Thermohaline Circulation Coupled Model Intercomparison Project” (UKTHCMIP) of the RAPID programme of the Natural Environment Research Council (NERC), under grants NERC NE/C509366/1 and NE/C522268/1. Data from UKTHCMIP are available from the British Atmospheric Data Centre. Data from the RAPID-WATCH MOC monitoring project are funded by the NERC and are available from [www.noc.soton.ac.uk/rapidmoc](http://www.noc.soton.ac.uk/rapidmoc). We acknowledge the CMIP3 modelling groups for making their model output available as, the Program for Climate Model Diagnosis and Intercomparison (PCMDI) for collecting and archiving this data, and the WCRP’s Working Group on Coupled Modelling (WGCM) for organizing the model data analysis activity. The WCRP CMIP3 multi-model dataset is supported by the Office of Science, US Department of Energy. Jonathan Gregory was partly supported by the Joint DECC and Defra Integrated Climate Programme, DECC/Defra (GA01101).

Edited by: J. Schröter

## References

- Anderson, D. L. T. and Corry, R. A.: Ocean response to low frequency wind forcing with application to the seasonal variation in the Florida Straits-Gulf Stream transport, *Prog. Oceanogr.*, 14, 7–40, 1985.
- Anderson, D. L. T. and Killworth, P. D.: Spin-up of a stratified ocean with topography, *Deep-Sea Res.*, 24, 709–732, 1977.
- Atkinson, C. P., Bryden, H. L., Hirschi, J. J.-M., and Kanzow, T.: On the seasonal cycles and variability of Florida Straits, Ekman and Sverdrup transports at 26° N in the Atlantic Ocean, *Ocean Sci.*, 6, 837–859, doi:10.5194/os-6-837-2010, 2010.
- Baehr, J., Cunningham, S., Haak, H., Heimbach, P., Kanzow, T., and Marotzke, J.: Observed and simulated estimates of the meridional overturning circulation at 26.5° N in the Atlantic, *Ocean Sci.*, 5, 575–589, doi:10.5194/os-5-575-2009, 2009.
- Biastoch, A., Böning, C. W., Getzlaff, J., Molines, J.-M., and Madec, G.: Mechanisms of interannual – decadal variability in the meridional overturning circulation of the mid-latitude North Atlantic Ocean, *J. Climate*, 21, 6599–6615, doi:10.1175/2008JCLI2404.1, 2008.
- Bigg, G. R. and Wadley, M. R.: Millennial changes in the oceans: an ocean modeller’s viewpoint, *J. Quaternary Sci.*, 16, 309–319, 2001.
- Bingham, R. J., Hughes, C. W., Roussenov, V., and Williams, R. G.: Meridional coherence of the North Atlantic meridional overturning circulation, *Geophys. Res. Lett.*, 34, L23606, doi:10.1029/2007GL031731, 2007.
- Blaker, A. T., Sinha, B., Wallace, C., Smith, R., and Hirschi, J. J.-M.: A description of the FORTE 2.0 coupled climate model, *Geosci. Model Dev.*, in preparation, 2011.
- Bleck, R.: An oceanic general circulation model framed in hybrid isopycnic-cartesian coordinates, *Ocean Model.*, 37, 55–88, 2002.
- Bower, A. S., Lozier, M. S., Gary, S. F., and Böning, C. W.: Interior pathways of the North Atlantic meridional overturning circulation, *Nature*, 459, 243–247, doi:10.1038/nature07979, 2009.
- Bryden, H. L., Mujahid, A., Cunningham, S. A., and Kanzow, T.: Adjustment of the basin-scale circulation at 26° N to variations in Gulf Stream, deep western boundary current and Ekman transports as observed by the Rapid array, *Ocean Sci.*, 5, 421–433, doi:10.5194/os-5-421-2009, 2009.
- Chidichimo, M. P., Kanzow, T., Cunningham, S. A., Johns, W. E., and Marotzke, J.: The contribution of eastern-boundary density variations to the Atlantic meridional overturning circulation at 26.5° N, *Ocean Sci.*, 6, 475–490, doi:10.5194/os-6-475-2010, 2010.
- Collins, M., Botzet, M., Carril, A. F., Drange, H., Jouzeau, A., Latif, M., Masina, S., Otteraa, O. H., Pohlmann, H., Sorteberg, A., Sutton, R. T., and Terray, L.: Interannual to decadal climate predictability in the North Atlantic: a multimodel-ensemble study, *J. Climate*, 19, 1195–1202, 2006.
- Cunningham, S. A. and Marsh, R.: Observing and modelling challenges in the Atlantic MOC. *Wiley Interdisciplinary Reviews: Climate Change*, 1(2), 180–191, 2010.
- Cunningham, S. A., Kanzow, T., Rayner, D., Baringer, M. O., Johns, W. E., Marotzke, J., Longworth, H. R., Grant, E. M., Hirschi, J. J.-M., Beal, L. M., Meinen, C. S., and Bryden, H.: Temporal variability of the Atlantic meridional overturning circulation at 26.5° N, *Science*, 317, 935–938, 2007.
- Dong, B.-W. and Sutton, R. T.: The dominant mechanisms of variability in Atlantic ocean heat transport in a coupled ocean-atmosphere GCM, *Geophys. Res. Lett.*, 28, 2445–2448, 2001.
- Dong, S., Garzoli, S. L., Baringer, M. O., Meinen, C. S., and Goni, G. J.: Interannual variations in the Atlantic meridional overturning circulation and its relationship with the net northward heat transport in the South Atlantic, *Geophys. Res. Lett.*, 36, L20606, doi:10.1029/2009GL039356, 2009.
- Edwards, N. R. and Marsh, R.: Uncertainties due to transport-parameter sensitivity in an efficient 3-D ocean climate model, *Clim. Dynam.*, 24, 415–433, 2005.
- Ganachaud, A. and Wunsch, C.: Large scale ocean heat and freshwater transports during the World Ocean Circulation Experiment, *J. Climate*, 16, 696–705, 2003.
- Gordon, C., Cooper, C., Senior, C. A., Banks, H., Gregory, J. M., Johns, T. C., Mitchell, J. F. B., and Wood, R. A.: The simulation of SST, sea ice extents and ocean heat transports in a version of the Hadley Centre coupled model without flux adjustments, *Clim. Dynam.*, 16, 147–168, doi:10.1007/s003820050010, 2000.
- Gregory, J. M., Dixon, K. W., Stouffer, R. J., Weaver, A. J., Driesschaert, E., Eby, M., Fichet, T., Hasumi, H., Hu, A., Jungclaus, J. H., Kamenkovich, I. V., Levermann, A., Montoya, M., Murakami, S., Nawrath, S., Oka, A., Sokolov, A. P., and Thorpe, R. B.: A model intercomparison of changes in the Atlantic thermohaline circulation in response to increasing atmospheric CO<sub>2</sub> concentration, *Geophys. Res. Lett.*, 32, L12703, doi:10.1029/2005GL023209, 2005.
- Griffies, S. M., Biastoch, A., Böning, C., Bryan, F., Danabasoglu, G., Chassignet, E. P., England, M. H., Gerdes, R., Haak, H., Hallberg, R. W., Hazeleger, W., Jungclaus, J., Large, W. G., Madec, G., Pirani, A., Samuels, B. L., Scheinert, M., Sen Gupta, A., Severijns, C. A., Simmons, H. L., Treguier, A. M., Winton, M., Yeager, S., and Yin, J.: Coordinated Ocean-ice Reference Experiments (COREs), *Ocean Model.*, 26, 1–46, 2009.
- Hodson, D. L. R. and Sutton, R. T.: The impact of model resolution on MOC adjustment in a coupled climate model, *Clim. Dynam.*, in preparation, 2011.
- Hirschi, J. J.-M., Baehr, J., Marotzke, J., Stark, J., Cunningham, S., and Beismann, J.-O.: A monitoring design for the Atlantic

- meridional overturning circulation, *Geophys. Res. Lett.*, 30, 1413, doi:10.1029/2002GL016776, 2003.
- Jayne, S. R. and Marotzke, J.: The dynamics of ocean heat transport variability, *Rev. Geophys.*, 39, 385–411, 2001.
- Johns, W. E., Baringer, M. O., Beal, L. M., Cunningham, S. A., Kanzow, T., Bryden, H. L., Hirschi, J. J.-M., Marotzke, J., Meinen, C. S., Shaw, B., and Curry, R.: Continuous, array-based estimates of Atlantic ocean heat transport at 26.5° N, *J. Climate*, 24, 2429–2449, doi:10.1175/2010JCLI3997.1, 2011.
- Johnson, H. L. and Marshall, D. P.: A theory for the surface Atlantic response to thermohaline variability, *J. Phys. Oceanogr.*, 32, 1121–1132, 2002.
- Jones, C., Gregory, J. M., Thorpe, R., Cox, P., Murphy, J., Sexton, D., and Valdes, P.: Systematic optimisation and climate simulations of FAMOUS, a fast version of HadCM3, *Clim. Dynam.*, 25, 189–204, 2005.
- Kanzow, T., Cunningham, S. A., Rayner, D., Hirschi, J. J.-M., Johns, W. E., Baringer, M. O., Bryden, H. L., Beal, L. M., Meinen, C. S., and Marotzke, J.: Observed flow compensation associated with the MOC at 26.5° N in the Atlantic, *Science*, 317, 938–941, 2007.
- Kanzow, T., Johnson, H., Marshall, D., Cunningham, S. A., Hirschi, J. J.-M., Mujahid, A., Bryden, H. L., and Johns, W. E.: Basin-wide integrated volume transports in an eddy-filled ocean, *J. Phys. Oceanogr.*, 39, 3091–3110, 2009.
- Kanzow, T., Cunningham, S. A., Johns, W. E., Hirschi, J. J.-M., Marotzke, J., Baringer, M. O., Meinen, C. S., Chidichimo, M. P., Atkinson, C., Beal, L. M., Bryden, H. L., and Collins, J.: Seasonal variability of the Atlantic meridional overturning circulation at 26.5° N, *J. Climate*, 23, 5678–5698, doi:10.1175/2010JCLI3389.1, 2010.
- Keenlyside, N. S., Latif, M., Jungclauss, J., Kornbluh, L., and Roeckner, E.: Advancing decadal-scale climate prediction in the North Atlantic sector, *Nature* 453, 84–88, 2008.
- Klinger, B. A. and Marotzke, J.: Meridional heat transport by the subtropical cell, *J. Phys. Oceanogr.*, 30, 696–705, 2000.
- Knight, J. R., Allan, R. J., Folland, C. K., Vellinga, M., and Mann, M. E.: A signature of persistent natural thermohaline circulation cycles in observed climate, *Geophys. Res. Lett.*, 32, L20708, doi:10.1029/2005GL024233, 2005.
- Lee, T. and Marotzke, J.: Seasonal cycles of meridional overturning and heat transport of the Indian Ocean, *J. Phys. Oceanogr.*, 28, 923–943, 1998.
- Lenton, T. M., Marsh, R., Price, A. R., Lunt, D. J., Aksenov, Y., Annan, J. D., Cooper-Chadwick, T., Cox, S. J., Edwards, N. R., Goswami, S., Hargreaves, J. C., Harris, P. P., Jiao, Z., Livina, V. N., Payne, A. J., Rutt, I. C., Shepherd, J. G., Valdes, P. J., Williams, G., Williamson, M. S., and Yool, A.: Effects of atmospheric dynamics and ocean resolution on bi-stability of the thermohaline circulation examined using the Grid ENabled Integrated Earth system modelling (GENIE) framework, *Clim. Dynam.*, 29, 591–613, 2007.
- Lozier, M. S., Roussenov, V., Reed, M. S. C., and Williams, R. G.: Opposing decadal changes for the North Atlantic meridional overturning circulation, *Nat. Geosci.*, 3, 728–734, doi:10.1038/ngeo947, 2010.
- Marsh, R., de Cuevas, B. A., Coward, A. C., Jacquin, J., Hirschi, J. J.-M., Aksenov, Y., George Nurser, A. J., and Josey, S. A.: Recent changes in the North Atlantic circulation simulated with eddy-permitting and eddy-resolving ocean models, *Ocean Model.*, 28, 226–239, 2009.
- Meehl, G. A., Stocker, T. F., Collins, W. D., Friedlingstein, P., Gaye, A. T., Gregory, J. M., Kitoh, A., Knutti, R., Murphy, J. M., Noda, A., Raper, S. C. B., Watterson, I. G., Weaver, A. J., and Zhao, Z.-C.: Global Climate Projections, in: *Climate Change 2007: The Physical Science Basis, Contribution of Working Group I to the Fourth Assessment Report of the Intergovernmental Panel on Climate Change*, edited by: Solomon, S., Qin, D., Manning, M., Chen, Z., Marquis, M., Averyt, K. B., Tignor, M., and Miller, H. L., Cambridge University Press, Cambridge, United Kingdom and New York, NY, USA, 2007.
- Megann, A. P., New, A. L., Blaker, A. T., and Sinha, B.: The sensitivity of a coupled climate model to its ocean component, *J. Climate*, 23, 5126–5150, 2010.
- Pacanowski, R. C.: MOM 1 Documentation Users Guide and Reference Manual GFDL Ocean Technical Report, Geophysical Fluid Dynamics Laboratory, NOAA, Princeton, USA, 1990.
- Schmittner, A., Latif, M., and Schneider, B.: Model projections of the North Atlantic thermohaline circulation for the 21st century assessed by observations, *Geophys. Res. Lett.*, 32, L23710, doi:10.1029/2005GL024368, 2005.
- Shaffrey, L. C. and Sutton, R. T.: The interannual variability of energy transports over and in the Atlantic Ocean in a coupled climate model, *J. Climate*, 17, 1433–1448, 2004.
- Shaffrey, L. C., Stevens, I., Norton, W. A., Roberts, M. J., Vidale, P. L., Harle, J. D., Jrrar, A., Stevens, D. P., Woodage, M. J., Demory, M. E., Donners, J., Clark, D. B., Clayton, A., Cole, J. W., Wilson, S. S., Connolley, W. M., Davies, T. M., Iwi, A. M., Johns, T. C., King, J. C., New, A. L., Slingo, J. M., Slingo, A., Steenman-Clark, L., and Martin, G. M.: UK-HiGEM: The new UK High resolution Global Environment Model. Model description and basic evaluation, *J. Climate*, 22, 1861–1896, 2009.
- Sime, L., Stevens, D. P., Heywood, K. J., and Oliver, K. I. C.: A decomposition of the Atlantic meridional overturning, *J. Phys. Oceanogr.*, 36, 2253–2270, 2006.
- Smith, R. S., Gregory, J. M., and Osprey, A.: A description of the FAMOUS (version XDBUA) climate model and control run, *Geosci. Model Dev.*, 1, 53–68, doi:10.5194/gmd-1-53-2008, 2008.
- Stouffer, R. J., Yin, J., Gregory, J. M., Dixon, K. W., Spelman, M. J., Hurlin, W., Weaver, A. J., Eby, M., Flato, G. M., Hasumi, H., Hu, A., Jungclauss, J. H., Kamenkovich, I. V., Levermann, A., Montoya, M., Murakami, S., Nawrath, S., Oka, A., Peltier, W. R., Robitaille, D. Y., Sokolov, A., Vettoretti, G., and Webber, S. L.: Investigating the causes of the response of the thermohaline circulation to past and future climate changes, *J. Climate*, 19, 1365–1387, 2006.
- Vellinga, M. and Wood, R. A.: Global climatic impacts of a collapse of the Atlantic thermohaline circulation, *Climatic Change*, 54, 251–267, 2002.
- Weaver, A. J., Eby, M., Wiebe, E. C., Bitz, C. M., Duffy, P. B., Ewen, T. L., Fanning, A. F., Holland, M. M., MacFadyen, A., Matthews, H. D., Meissner, K. J., Saenko, O., Schmittner, A., Wang, H., and Yoshimori, M.: The UVic Earth System Climate Model: Model description, climatology and application to past, present and future climates, *Atmos. Ocean*, 39, 361–428, 2001.
- Webb, D. J.: An ocean model code for array processor computers, *Comput. Geosci.*, 22, 569–578, 1996.

- Webb, D. J., de Cuevas, B. A., and Richmond C. S.: Improved advection schemes for ocean models, *J. Atmos. Ocean. Tech.*, 15, 1171–1187, 1998.
- Willis, J. K.: Can in situ floats and satellite altimeters detect long-term changes in Atlantic Ocean overturning?, *Geophys. Res. Lett.*, 37, L06602, doi:10.1029/2010GL042372, 2010.
- Wunsch, C.: Mass transport variability in an eddy-filled ocean, *Nat. Geosci.*, 1, 165–168, 2008.
- Zhang, R.: Latitudinal dependence of Atlantic meridional overturning circulation (AMOC) variations, *Geophys. Res. Lett.*, 37, L16703, doi:10.1029/2010GL044474, 2010.